17th World Conference on Earthquake Engineering, 17WCEE
Sendai, Japan - September 13th to 18th 2020

LAP-SPLICE DEVELOPMENT EFFECTS ON DEFORMATION CAPACITY OF R.C. ELEMENTS

S.J. Pantazopoulou[(1)], S.P. Tastani[(2)]

[(1)] *Professor of Civil Engineering, York University, Toronto, Canada, pantazo@yorku.ca*
[(2)] *Assist. Professor of Civil Engineering, Democritus University of Thrace, Greece, stastani@civil.duth.gr*

Abstract

The state of stress and strain that develops along lap-splices in the plastic hinge regions of reinforced concrete (r.c.) elements (i.e., columns and structural walls), subjected to lateral displacements such as would occur during earthquakes is explored in detail in the paper. Therefore, the field equations of bond along the lap splice of the longitudinal reinforcement are established and solved from first principles using simplified constitutive relationships for steel and for the reinforcement-to-concrete bond. In the formulation, important design variables such as the aspect ratio of the element span, the local effects of combined lateral drift and axial strain, and the corresponding stress resultants (flexural moment and axial load ratio) are considered. Using this solution, the sequence of cracking and subsequent failure modes occurring in flexural elements with lap-splices by considering the penetration of debonding along the lapped bars that starts from the ends of the lap splice, is demonstrated. The limitation that these failure modes impose on the drift capacity of the structural member is explored with reference to the geometric details on the lap splice, (length ℓ_o, bar diameter D_b, clear cover c, transverse reinforcement), the normalized shear strength demand, and the strain gradient over the span occurring as a result of lateral sway. A primary finding is that the crack width at the critical section, which determines the contribution of reinforcement pullout slip to the total member drift is controlled entirely by the bar in the splice-pair that is anchored in the foundation. It is shown from the mechanics of the bond problem that this bar behaves as an anchorage on both sides of the critical section, and thus, the drift capacity of the member depends on this bar's strain development capacity at the critical section. Thus, criteria need be prescribed to secure the development of post-yielding strain in the lower lapped bars, so that the nominal drift capacity of columns/shear walls may be regulated in seismic design. Cover spalling in the compression zone is an inevitable implication of slip in the tension reinforcement, which deteriorates bond and strain development in subsequent cycles under load reversal. Analytical estimations are also compared with experimental evidence obtained from published relevant tests on flexural specimens with lap-splices in the critical regions under combined lateral displacement reversals and overbearing axial load.

Keywords: Seismic design, deformation capacity, lateral drift, plastic hinge length, walls/columns, lap-splices

1. Introduction

Reinforcement anchorages and lap splices are considered a detailing requirement in conventional design, where the development length provided is designed to be able to support the bar yielding force. It is expected therefore, that reinforcement would yield at the critical sections, however the intensity of longitudinal strain is not considered explicitly in design. Routine flexural strength calculations of members bent in flexure are generally carried out with the requirement that the Axial Load and Moment combinations at the Ultimate Limit State (ULS) lie below the balanced state of failure, whereby acceptable bar strain magnitudes at the critical section would be in the range of 0.002 – 0.02. This strain range is theoretical, considering the rupture strain of the reinforcement as an upper limit; however, it is important to note that the rupture limit many never be realized in practice if the lap-splice/anchorage cannot support the development of such large strains.

Former studies [1-4] illustrated that when excessive post-yielding strains occur at the critical section of a member (at the face of the support during seismic excitation) then, strain penetration occurs both in the bar anchorage and in the shear span of the member. The implications of strain penetration are, 1) increased pullout rotation (i.e. a higher crack width in the tension side of the critical section) and 2) commensurate increased strains in the compression zone. This finding has been used to explain the propensity for cover crushing i.e. in the toe of slender walls under high drift demands (reconnaissance reports Chile 2010, Christchurch 2011 and [5]). It was found by studying the above finding, that the estimated compression strain increase may exceed by more than 30% the base design value, which in turn lengthens the required confined zone of the wall considering the extent of strain penetration of the longitudinal reinforcement [3]. An analytical investigation of the interaction between bond conditions of the primary reinforcement (bond-slip) and flexural action in shear span resulted in a more consistent definition of plastic hinge length in r.c. members, over which post-yielding strains have penetrated during seismic lateral deflection [4]. This in turn has implications on performance-based seismic design and assessment of r.c. members.

Common practice in r.c. columns/walls is the development of lap splices of longitudinal reinforcement at the base. A variety of lateral load tests conducted on r.c. elements indicate that these lap splices have a far reaching effect on strength and deformation capacity. As early as 1992 in [6] it was shown that lap splices located in the plastic hinge regions of flexural members inevitably fail by pullout regardless of the splice length and the presence of sufficient stirrup arrangement: even cases with a spliced length of ℓ_o=40D_b (D_b the bar size) failed in that mode, a circumstance followed by a severe strength loss at a drift of 2%. In fact, only hooked lap-splices (i.e. splices that contain a control mechanism against bar slippage) were able to preclude premature failure and demonstrated a response commensurate to that of members reinforced with continuous bars. Villalobos et al. [7] reported similar findings from wall tests: even in the case of extended lap splices (ℓ_o=60D_b) drift capacity of the wall was reduced by 30%, and was marked by strain concentration in the reinforcement at the critical section. In fact it was shown that deformation capacity of r.c. walls is limited by the resisting mechanism that controls its failure mode [3]: in particular, the strain development capacity of the reinforcement controls the drift at failure, as penetration of strain spreads in the shear span from the critical region. The wall aspect ratio was also an important parameter in that respect, through its effect on the gradient of strain demands in that zone. Evaluation of available test evidence by [8] illustrated that well-confined lap splices relocate the plastic hinge above the lap splice. On the other hand, lap-splices of adequate length to develop the bar force, but insufficiently confined, attain the peak force but their deformation capacity is significantly reduced; in the absence of confinement short lap-splices fail prior to development of bar yielding with longitudinal splitting of cover. In terms of seismic performance of walls with lap-splices, it was shown that important parameters are, the fraction of the shear span length covered by the lap splice, and the amount of available confinement over ℓ_o. Both parameters affect the strain development capacity of the lap-spliced reinforcement and the associated plastic rotation capacity of the member.

1.1 The state of strain in the lap-splice region of a r.c. element under lateral drift

Attainment of flexural yielding in r.c. column/wall sections is followed by the post-yielding plateau owing to the large plastic rotations that occur in the plastic hinge region adjacent to the support. In light of the

relationship between bond stress f_b and the gradient of bar stress distribution df_s/dx [i.e. $f_b=D_b/4\cdot(df_s/dx)$], it follows that once the longitudinal bars enter the yield plateau, the term df_s/dx becomes zero if the reinforcement is elastoplastic, or very small in case of strain hardening reinforcement. Thus yielding of a bar embedded in concrete is synonymous with the destruction of interfacial bond which leads to spreading of bar reinforcement yielding (yield penetration) away from the critical section and into the anchorage. The length of reinforcement over which bar strains exceed the yielding limit can't be defined by the gradient of externally applied moments (i.e., where $M>M_y$) as would be generally assumed in design practice. Rather, bar strains in that region are controlled by the bond-slip bar-strain interaction. The reduction of the available development length and thus the strain development capacity of the reinforcement affects the plastic rotation capacity of the r.c. member. Failure at the top of the splice at the compression side of the wall cross section due to the ramming action of the a-bars (for definition see §2.1) on the concrete cover has been reported, causing side splitting at a drift 0.25% [8-9]. In that study it was observed that at a drift of 0.35% side splitting was extended over the entire ℓ_o. All deformation after 0.5% drift (drop of resistance) occurred at the top of the splice, by opening of a horizontal crack. Beyond this point, no additional cracks formed, whereas the pre-existing ones above the lap splices progressively reduced their width with increasing drift. In [10] is also mentioned that the drift ratio was reduced up to 40% as compared to that of specimens with continuous reinforcement. In any case yielding was near 0.5 to 0.7% drift ratio. No damage was observed beyond the splice, however in specimen with $\ell_o=40D_b$ a splitting crack along ℓ_o caused the lateral concrete cover on one side of the wall to spall off.

In this paper the solution of the bond equation over ℓ_o occurring at the r.c. member base is formulated considering cover debonding after bar yielding and spread of inelasticity in the lap splice. The objective is to determine the available strain development capacity of the lap splice, and from there the lap-splice pullout effect on the member's rotation capacity. Analytical results are explored to identify the implications of the phenomena studied on the detailing requirements in the plastic hinge regions with inadequately confined ℓ_o.

2 Bond-slip mechanics in a lap splice

Consider a cantilever r.c. member of height L_s with cross section $h \times b$ under monotonically increasing lateral load and constant axial compression (simulating earthquake effects, Fig. 1a). Longitudinal reinforcing bars (diameter of D_b) are considered to be spliced into the shear span for a length ℓ_o and anchored in the adjacent footing with an end hook (it is assumed that the presence of a hook is equivalent to increasing the straight anchorage length L_b by an amount of $12.5D_b$ [11]; thus, the effective anchorage length is taken as $L_b^{eq}=L_b+12.5D_b$). The process of an anchored reinforcing bar inelastic strain penetration within L_b^{eq} with increasing drift demand was already demonstrated in [1-2].

In the analysis, a point of reference is the moment - curvature relationship (M_o-ϕ_o) that develops at milestone points along the member height (considering concrete tension cracking and assuming kinematics of plane sections remaining plane and normal to the member axis): from this, the moment – bar tensile strain (M_o - ε_o) of the remotest bar-pair may be obtained (Fig. 1b). Such milestone points are, the critical sections at the ends of the lap splice where flexural cracks have been observed to occur first, owing to the stiffness discontinuity effected by the change in the amount of reinforcement (area of a lapped pair vs of a single bar at the ends of ℓ_o, thereby increasing the sectional stiffness before first cracking; thus cracking occurs exactly at the transition point [8-9]). It is common practice in this sectional analysis for each lapped pair to be treated as a single bar. For simplicity of calculations and with no loss of generality, the M_o - ε_o curve is approximated by a polynomial function in the remainder. This function is used to obtain the strain in the bars given the acting moment at a cracked section location (symbolized as $M\rightarrow\varepsilon$), as well as the reverse ($\varepsilon\rightarrow M$). Note that at a cracked location there is no strain compatibility between bar and concrete: the concrete strain is zero, whereas the bar strain increases locally on account of the cracked section equilibrium. Clearly, strain compatibility is not recovered immediately adjacent to the crack, but requires a non-trivial distance from the crack till the two materials may be considered to be compatible again. Over that distance, the state of strain in the bars is controlled by bond-slip, and cannot be obtained from M_o - ε_o relationship.

2.1 Strain development in the lapped bars

In the resulting sections, the notation used when referring to the bar response indices is as follows: the first digit (i=1,2) corresponds to numbering of tension bar pairs starting from the sections' extreme fiber and proceeding towards the neutral axis (n.a.), and the second digit, (j=a or e) denotes the bar in the lap-spliced pair that is anchored in the footing or is developed in the shear span, respectively (Fig. 1a,c).

The flexural moment at a distance x from the support is estimated with reference to the flexural moment at the support, M_o, as $M(x) = M_o \cdot (1 - x/L_s)$. Moment M_o corresponds to the global bar tensile strain ε_o at x=0, which corresponds to the strain of the remotest tension lap splice from the center of the cross section, and specifically, to the bar of the lap-spliced pair that is anchored in the footing, i.e., $\varepsilon_o = \varepsilon_{1.a}|_{x=0}$ (Fig. 1c). The strains in all the other anchored bars of the cross section, i.e., $\varepsilon_{2.a}|_{x=0}$, may be calculated considering curvature ϕ_o and the distance, y_i^{na}, of the point considered from neutral axis, as follows: $\varepsilon_{i.a}|_{x=0} = \phi_o \cdot y_i^{na}$ where $\phi_o = \varepsilon_o / y_1^{na}$. At x=0, the associated e-bars in the shear span have zero strain (i.e., $\varepsilon_{1.e}|_{x=0} = \varepsilon_{2.e}|_{x=0} = 0$). Similarly, at the cut-off point of the lap-splice, $x = \ell_o$, the moment is $M_{\ell o} = M_o \cdot (1 - \ell_o / L_s)$. Here, after cracking, the global strain $\varepsilon_{\ell o}$ coincides with the strain of the developed bar of the remotest pair as $\varepsilon_{1.e}|_{x=\ell o} = \varepsilon_{\ell o}$ whereas

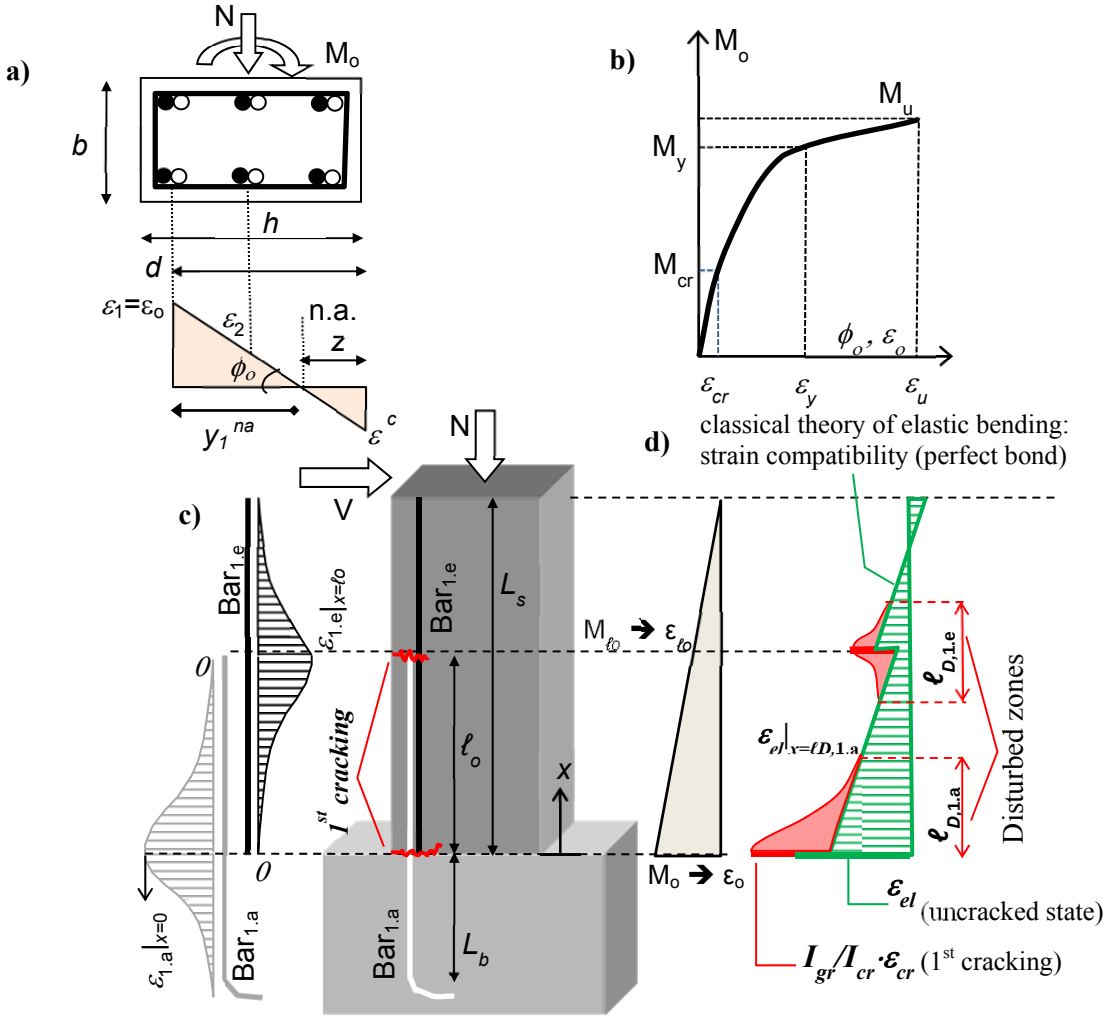

Figure 1 - a) Notation of strain at the critical cross section (base). b) Graphs depicting Moment – curvature – and Moment vs. steel tensile strain of the anchored bar of the remotest tension pair at base. c) Notional strain distributions among the paired bars. d) Bar strain distribution at uncracked state (green) and local strain increase (red) upon first cracking and state of strain at the ends of the lap splice.

the strain of the paired anchored bar is diminished, $\varepsilon_{1.a}|_{x=\ell o}=0$. Given the curvature $\phi_{\ell o}$, it is straightforward to calculate the strain $\varepsilon_{2.e}$ from $\varepsilon_{\ell o}$. For simplicity, the lap-spliced pairs in compression are assumed to act as continuous reinforcing bars. However, as mentioned in the preceding, the end point of lap-splices when placed in the compression zone of the section span rams into the cover in every cycle, and it is expected to induce cover spalling as is usually reported in compression-lap experiments [11-12].

2.2 Formation of flexural cracks at the ends of splice

Prior to cracking, the moment of inertia I of the member cross section is higher within the lapped region than outside, due to the double amount of bar reinforcement area. With increasing applied lateral displacement at the member tip, the flexural moment reaches cracking value first at x=0, and therefore, the critical section occurs at, or near the face of the support. Immediately following the formation of the first flexural crack, the strain in the a-bars increases suddenly, as it is amplified by the ratio I_{gr}/I_{cr}, where I_{gr} and I_{cr} are the uncracked and cracked moment of inertia respectively. A short distance away from the critical section, at $x=\Delta x$, the flexural moment $M(x)$ is less than the cracking moment M_{cr}. [$M_{cr}=(f_{ct}+N/A_g)\cdot I_{gr}/(0.5h)$, where f_{ct} is the tensile strength of concrete, N the axial load -compression positive-, $A_g= b\cdot h$ is the cross-section area, and h is the cross-sectional height.] However the strain in the a-bar can no longer be obtained from the M_o-ε_o diagram (Fig. 1b), because it takes a certain distance from the cracked section before compatibility of concrete and bar strains may be reinstated; this distance is referred to hereon as disturbed zone $\ell_{D,1.a}$ (see Fig. 1d). Over the disturbed zone, bar strain is governed by the solution of the differential equation of bond and slip (Appendix A, also [4]). Slip of the a-bar is accommodated as crack width of the critical section.

According to the bar strain distribution (red curve, Fig. 1d), in region $\ell_{D,1.a}$ bond action dominates bar 1.a strain response whereas bar 1.e is almost inactive. At $x=\ell_o$, where the abrupt change in reinforcement area occurs, the e-bar strain distribution presents a local jump on account of the different I_{gr} value below and above that point. When a flexural crack forms at that position, it evokes similar bond effects to e-bar as described in the preceding for the a-bar: bond governs the magnitude of strain in the e-bar over a disturbed zone $\ell_{D,1.e}$, but of lesser extent than $\ell_{D,1.a}$ [because $M(x=\ell_o)=M_{cr}(1-\ell_o/L_s)$]. Strain compatibility between concrete and the bars may only be claimed in the remaining segments as shown by the green line in Fig. 1d.

2.3 Propagation of splitting from the ends of splice - reduction of the effective splice length

After formation of the end cracks in the lap-splice, the mechanics of bond failure and the sequence of occurrence follow the solution of a similar problem obtained for splices under constant flexural moment [13]: it was shown that after flexural cracking occurs at both ends of ℓ_o, formation of further intermediate flexural cracks within ℓ_o is possible if only it is simultaneously accompanied by instant splitting failure over the spliced pair (unzipping phenomenon), starting from the ends of the lap-splice and propagating inwards up until the position of the new flexural cracks. This important compatibility requirement has been explained as follows: a flexural crack in a splice region crosses the pair of the spliced bars, where the a-bar is highly stressed and the e-bar is stressed by the complementary amount, so that the sum of the two stresses equals the bar stress input– bar force at that point is obtained from the ratio of moment divided by the internal lever arm. Loss of bond along the a-bar leads to increased slip (which may be calculated from integration of bar strains), and therefore widening of the flexural crack. The adjacent e-bar needs to also accommodate the same crack width. This compatibility requirement cannot be satisfied in light of the fact that the e-bar's strains of lesser magnitude do not produce the same amount of slip as the a-bar. The only way that this geometric requirement may be satisfied is if bond is eliminated over a certain interval bounded by the former and the newly originated flexural crack for both bars. Elimination of bond occurs by cover splitting failure. From that point on, the splice strength is developed only in the remaining intact undamaged length. Therefore lap splice strength is gradually diminished by penetration of strain starting from the ends of the splice and propagating inwards. Extending this finding to the cantilever paradigm means that strain penetration will occur into the debonded region denoted by $\ell_{1.a}^{cr2}$ for the a-bar whereas strain will be released in the e-bar at that region (bottom end of splice); this is schematically shown in Fig. 2.

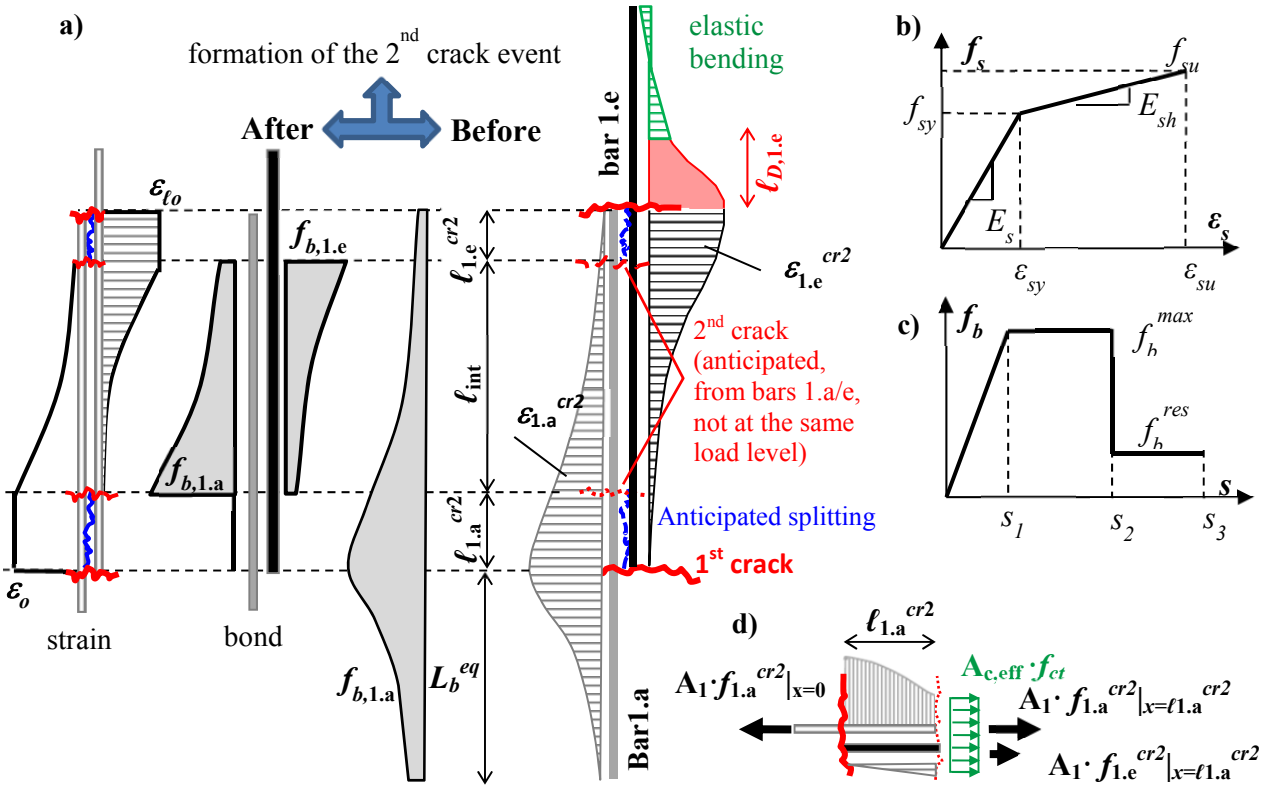

Figure 2 – a) Depiction of progressive bond failure upon anticipation of inner flexural cracking and bar strain and bond stress distributions after formed inner cracking. b) Stress-strain law of steel reinforcing bar. c) Local bond - slip law. d) Equilibrium of internal forces for the anticipated 2nd flexural cracking.

2.4 Formation of intermediate flexural cracks in the lap splice

After crack formation in the ends of the splice length, each bar of the pair within ℓ_o behaves as an anchorage: each bar's strain must attenuate from the peak value at the crack down to zero at the tip of the splitting crack in the opposite end of the splice. For this to be possible bond stresses are being developed thus eliminating strain compatibility between bar and concrete in ℓ_o. The bond conditions in that region define the mode of strain attenuation thus regulating accordingly the arm j_d of the sectional forces in resisting the moment gradient and the associated shear force V:

$$V = dM(x)/dx = A_S \cdot d(j_d \cdot f_S)/dx = A_S j_d \cdot \overbrace{(df_S/dx)}^{\approx 0} + A_S f_S (dj_d/dx) \quad (1)$$

Thus, as debonding proceeds, for constant bar stress (yielded) the moment gradient which is a result of equilibrium, requires a change in the internal lever arm which is directly proportional to the magnitude of shear – a finding that underscores the function of a strut and tie mechanism in the disturbed zone.

To find the location of the second flexural crack event inside the lap-splice, the moment gradient must be also considered. Here, the contingent position of the event is at a distance $x=\ell_{1.a}^{cr2}$ from the most stressed splice end at the base of the member. Just before crack formation, which will first cross the remotest pairs of lapped bars in the tension zone of the cross section, the concrete stress in the cover engaged by bond is equal to its tensile strength property, f_{ct} (Fig. 2d) and the a-bar strain must exceed the cracking limit at that position, $\varepsilon_{cr,s}$ (for its definition see App. A). (In the case of walls, these pairs are the most critical for initiation of splice failure and signal the strength degradation.) Considering that the total reinforcement area of the remotest layer of lapped bars is $A_1=n\cdot\pi D_b^2/4$, where n is the number of lapped pairs at that location, the requirement of equilibrium of forces over the interval $\ell_{1.a}^{cr2}$ takes the form:

$$A_1 \cdot f_{1.a}^{cr2}\,|_{x=0} = A_{c,eff}\, f_{ct} + A_1 \cdot \left(f_{1.a}^{cr2} + f_{1.e}^{cr2}\right)|_{x=\ell_{1.a}^{cr2}} \Rightarrow\; A_1 \cdot \left(f_{1.a}^{cr2}\,|_{x=0} - f_{1.a}^{cr2}\,|_{x=\ell_{1.a}^{cr2}} \right) = A_{c,eff}\, f_{ct} + A_1 \cdot f_{1.e}^{cr2}\,|_{x=\ell_{1.a}^{cr2}} \quad (2a)$$

where, $A_{c.eff}$ is the area of concrete effectively engaged in tension by the remotest pairs; this is approximated as $A_{c.eff} = [b\cdot(2c+D_b) - 2\cdot A_1]$, where c is the clear cover. In Eq. (2a), the stress difference ($f_{1.a}{}^{cr2}|_{x=0}$ - $f_{1.a}{}^{cr2}|_{x=\ell_{1.a}{}^{cr2}}$) between 1st and 2nd crack for bars 1.a is supported by the associated bond stress $f_{b,1.a}$ along $\ell_{1.a}{}^{cr2}$. For bar 1.e in $\ell_{1.a}{}^{cr2}$, stress is reduced from $f_{1.e}{}^{cr2}|_{x=\ell_{1.a}{}^{cr2}}$ to zero due to bond $f_{b,1.e}$. Thus Eq. (2a) becomes:

$$n\cdot \pi D_b \int_0^{\ell_{1.a}^{cr2}} f_{b,1.a}(x)dx = A_{c,eff}\, f_{ct} + n\cdot \pi D_b \int_0^{\ell_{1.a}^{cr2}} f_{b,1.e}(x)dx \quad (2b)$$

For the implementation of Eqs. (2), the field equations for the bond problem over ℓ_o need to be solved; considering that the bond splice problem is identical to that of an anchorage [1-2], the solution is summarized in the Appendix B. Equation (2b) defines the position of the 2nd flexural crack inwards with the condition (as already stated) of instant cover splitting just upon the occurrence of the event; cover splitting is considered as an event that eliminates bond over $\ell_{1.a}{}^{cr2}$. The consequence is that the bar strain $\varepsilon_o = \varepsilon_{1.a}|_{x=0}$ is now transferred to the position $x=\ell_{1.a}{}^{cr2}$. in the absence of any other resisting mechanism against irrepressible unzipping - At that position (i.e., $x=\ell_{1.a}{}^{cr2}$), where moment is lower than M_o, the equilibrium of internal forces may be claimed by lowering their arm jd [Eq. (1)].

If transverse reinforcement of proper anchorage is present along $\ell_{1.a}{}^{cr2}$, then it is able to partly reduce the strain ε_o at $x=\ell_{1.a}{}^{cr2}$ due to its contribution to bond residual resistance f_b^{res} [11,14] as $\varepsilon_{1.a}|_{x=\ell 1.a}{}^{cr2} = \varepsilon_o - 4f_b^{res}\ell_{1.a}{}^{cr2}/(D_b E_s)$. At that cracked position, given the reinforcement tensile force from flexural analysis and the share undertaken by the 1.a bar due to $\varepsilon_{1.a}|_{x=\ell 1.a}{}^{cr2}$, the complementary force may be found and thus the strain of the 1.e bar. This state alters the boundary conditions of the 1.e bar; now it behaves as an anchorage only into $\ell_{1.a}{}^{cr2}$ whereas in the remaining length ℓ_o-$\ell_{1.a}{}^{cr}$, given the known strains at its end (of different magnitude), bond needs to change direction at a distance x_m from $x=\ell_{1.a}{}^{cr2}$ [13]. This phenomenon is the familiar tension stiffening effect, and it is introduced in the model solution by the requirement that the bar axial strain distribution presents an extreme at position x_m, as $d\varepsilon_{1.e}(\underline{x})/d\underline{x}\,|_{x=xm}=0$ ($\underline{x}$ is measured from $\ell_{1.a}{}^{cr}$, thus at $x=\ell_{1.a}{}^{cr2}$ it is $\underline{x}$=0). Apparently as higher stress is transmitted from 1.a to the 1.e bar, the latter may be responsible for flexural cracking too near the end ℓ_o. This behavior is shown in the next section.

The sequence of crack formation terminates when bond in the intact part of the splice, i.e. $\ell_{int}=\ell_o-\Sigma(\ell_{1.a}{}^{cr.n} + \ell_{1.e}{}^{cr.n})$, is no longer sufficient to transfer enough force to concrete so as to cause its overload and subsequent further cracking in tension (release of Eqs. 2). This stage is the stabilization of cracking. Thus, from the onset of crack-stabilization and upon further increase of the load, existing cracks begin to grow in terms of their own width; load increase depends only on the bond reserves in ℓ_{int}. Thus, at the limit, in calculating the drift capacity of the bar, it may be assumed that the bar extending from the foundation may be treated as a double anchorage, with the length in the shear span limited by ℓ_{int}.

3. Application of the proposed model to an experimental case study

The example considered was selected from the experimental literature [15]: The cantilever column specimen (named NS-X0) had a cross-section of 300x200mm (h x b), shear span L_s=1200mm, reinforced at corners with 4 bars of D_b=14mm, yielding stress f_{sy}= 460 MPa and splice length ℓ_o=40D_b =560 mm. Concrete compressive strength was 26 MPa with E_c=32 GPa. Stirrups of $D_{b,st}$=8mm and $f_{y,st}$=490MPa were spaced at S=100mm. The constant axial load was 282kN (v=0.2). According to the available data: all flexural cracks into ℓ_o had been formed up to a drift 0.75% (for load not exceeding 45kN, or a moment of 54kNm), two at the ends of the splice and two internal major cracks, one at 150mm (for both loading directions) and the other at 250/350mm from base. From drift 1% and beyond the e-bars were almost inactive whereas the a-bars were strained far beyond yielding (measurements at level x=100mm from base) and were practically inactive at the tail of ℓ_o for a length around 150-200mm. At drift 0.8% yielding of a-bars were reported and at 1% cover crushing was started. Also after yielding of the specimen (form flexural analysis, yielding was

estimated at around 52kN or 62 kN-m, Fig. 3b) progressive spalling of compression cover near the support occurred simultaneously with splitting of splice. The divergence among the ascending branches of load-drift envelopes in the two loading directions (Fig. 3a), being more pronounced at drift 1%, may be explained as follows: the onset of compression cover spalling in some extent during positive loading (blue curve, Fig. 3a) affected the bond of compression splices. At load reversal, being mobilized in tension, these splices had to rely on reduced cover resistance.

For the analysis bond strength was taken as f_b^{max}=9MPa and f_b^{res}=4.4MPa (s_1=0.2mm). The analysis is limited in presenting only the cracking induced by 1.a bar and the associated induced drift of the column.

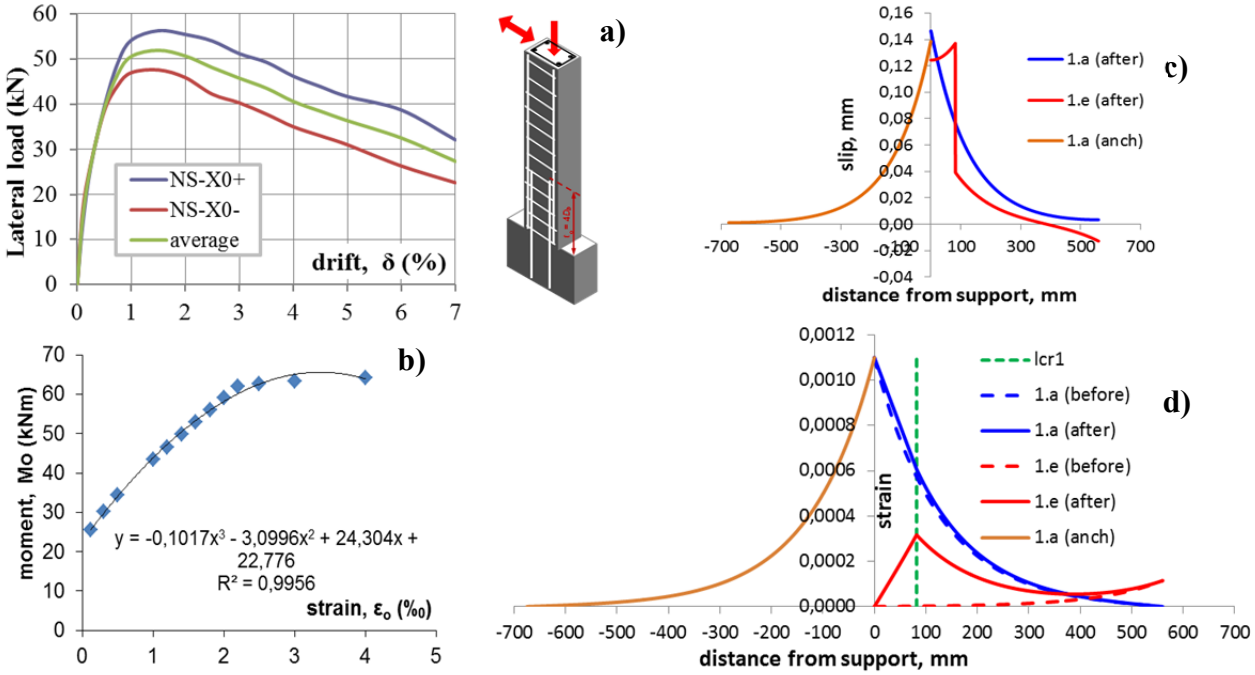

Figure 3. Analysis of NS-X0 [15]: a) experimental response, b) flexural analysis of cracked cross section, c) associated slip distribution after the event and d) strain distributions along the spliced bars before (dashed curves) and just after (solid curves) the formation of the internal crack, as well as along the anchorage.

More specifically, in Fig. 3c it is shown that at strain level ε_o=0.0011 (moment M_o=46kNm ➔ lateral load 38kN) an internal flexural crack is anticipated at $\ell_{1.a}^{cr2}$=82mm (for a lower bond strength, i.e. f_b^{max}=6MPa, cracking would be transferred, to occur at a higher distance and for a lower strain level); before cracking the paired bars have strain distributions as depicted by the dashed curves. Just after cracking (solid curves) the distribution of bar 1.e is drastically altered mainly as a result of the residual bond strength magnitude f_b^{res}; the lower the f_b^{res} is, the response approaches the one shown in Fig. 4, that means the bar 1.a undertakes the whole tensile force without transferring stress to bar 1.e. In Fig. 3d the slip distributions are shown along the splice and anchorage lengths after cracking; for this strain state, the sum of magnitudes of bar 1.a from splice and anchorage (assuming, for simplicity and with no loss of generality the same bond - slip law as in the splice) results to a crack opening (see Appendix B) as w_o=0.14+0.15=0.29mm and thus to a drift lumped rotation of the column as $\theta_{pull}=w_o/y_1^{na}$ =0.29/122=0.23% (note that from flexural analysis it has been found that the tension zone is, y_1^{na}=122mm, and compression zone z=143mm, and the effective height d=265mm). The drift due to flexural response is θ_{fl} =1/3ε_o/(d-x)L_s=0.36%. Thus, the total drift at this stage is θ=0.59%, a magnitude that matches the experimental response (see Fig. 3a); and about 38% of that amount is owing to pullout from both anchorage and shear span of the a-bar. Beyond that point, the strain development capacity of the a-bar completely controls the drift behavior of the structural member. As the cover strain in the compression zone increases, delamination of the cover reduces the bond strength of the compression bars, an event that dominates their development capacity upon reversal of the load. The total drift of the

member is then limited by the total strain that the a-bar may support at the critical section – this strain will be limited by the development capacity of either the anchorage or the a-bar extension in the shear span.

4. Conclusions

Pullout rotation resulting from yield penetration at the base of columns and walls is limited by the development capacity of the spliced bars at the base. If the amount of pullout slip that occurs at the member to footing interface is significant, then this also effects the development of increased compressive strains in the concrete cover of the compression zone [16]. Therefore, the length of the lap splices, determines the maximum drift level that may be attained prior to delamination of the concrete cover in the compression zone and the ensuing degradation of flexural strength, in a manner that is not understood in the literature. It was shown that the length of the splice is most critical, as cover splitting in the tension zone is unavoidable in the absence of pertinent external confinement. Splitting implies that it is no longer possible to anchor significant post-yielding forces in the absence of transverse reinforcement, and that a large fraction of the total deformation capacity of the member is driven by two-way pullout of the tension bars from the anchorage and the lap-zone respectively. This mechanism of behavior is not explicitly acknowledged in estimations of drift capacity of columns and walls in practical seismic assessment, particularly when considering existing construction. The mechanism of a strut and tie formation being a consequence of bond loss over the splitted spliced length is also illustrated from first principles.

5. References

[1] Tastani SP, Pantazopoulou SJ (2013a): Yield penetration in seismically loaded anchorages: effects on member deformation capacity. *Earthquake Structures*, **5**(5), 527-552.

[2] Tastani SP, Pantazopoulou SJ (2013b): Reinforcement-concrete bond: state determination along the development length. *ASCE Journal of Structural Engineering*, **139**(9), 1567-1581.

[3] Tastani SP, Pantazopoulou SJ (2015): Implications of yield penetration on confinement requirements of r.c. wall elements. *TechnoPress Earthquakes and Structures*, **9**(4).

[4] Megalooikonomou K, Tastani SP, Pantazopoulou SJ (2018): Effect of yield penetration on column plastic hinge length. *Elsevier Engineering Structures,* **156**, 161-174.

[5] Wallace JW, Moehle J (2012): Behavior and design of structural walls - Lessons from recent laboratory tests and earthquakes. *Int. Symp. on Engng. Lessons Learned from the 2011 Great East Japan Earthquake*, Tokyo, Japan.

[6] Yoshimura M, Tsumura K (1992): Test of reinforced concrete beams with lap splices at hinge region. *10th World Conference on Earthquake Engineering*, Madrid, Spain.

[7] Villalobos E, Escolano-Margarit D, Ramırez-Marquez AL, Pujol S (2017): Seismic response of reinforced concrete walls with lap splices. *Bull. Earthquake Eng.*, **15**:2079–2100.

[8] Almeida JP, Prodan O, Tarquini D, Beyer K (2017): Influence of lap splices on the deformation capacity of rc walls I: database assembly, recent experimental data, and findings for model development. *ASCE J.Str.Engrng.*, **143**(12).

[9] Lowes L, Lehman D, Birely A, Kuchma D, Marley K, Hart C (2012): Earthquake response of slender planar concrete walls with modern detailing. *Engineering Structures*, **43**,31–47

[10] Villalobos E, Pujol S (2014): Seismic Response of rc walls with lap splices. *10th U.S. National Conference on Earthquake Engineering: Frontiers of Earthquake Engineering* (10th USNCEE), Anchorage, Alaska.

[11] fib CEB-FIP (2010): fib Model Code 2010. Bulletin No. 65, Lausanne, Switzerland.

[12] Cairns J (1985): Strength of compression splices: a reevaluation of test data. *ACI Journal*, **82**(4), 510-516.

[13] Tastani SP, Brokalaki E, Pantazopoulou SJ (2015): State of bond along lap-splices. *ASCE J. Str. Engng,* **141**(10).

[14] Tastani SP, Pantazopoulou SJ (2010): Direct tension pullout bond test: experimental results. *ASCE J. Str. Engng*, **136**(6), 731-743.

[15] Göksu Ç. Seismic behaviour of RC columns with corroded plain and deformed reinforcing bars. PhD thesis, Dept. Civil Engineering, Istanbul Technical University, Turkey, 2012.

[16] Syntzirma DV, Pantazopoulou SJ, Aschheim M (2010): load history effects on deformation capacity of flexural members limited by bar buckling. *ASCE J. of Structural Engineering*, **136**(1),1-11.

Appendix A - From [4]: for the stage prior to the occurrence of first flexural cracking at x=0, the a-bar strain (green distribution, Fig. 1d) is estimated from the flexural analysis:

$$\varepsilon_{1.a}(x) = \frac{M_o \cdot (1\text{-}x/L_s)}{E_c \cdot I_{gr}} \cdot y_{cg} - \frac{N}{E_c \cdot A_g} \quad ; \quad y_{cg} = 0.5h - c - 0.5D_b \tag{A.1}$$

where E_c is the elastic modulus of concrete, I_{gr} and A_g are the moment of inertia and the uncracked cross section area, h is the section height and c the clear cover, y_{cg} is the distance of the centroid of a-bar to the centroid of cross-section. Upon cracking of the tension zone the bar strain experiences a significant jump to maintain equilibrium (Fig. 1d), even though the moment change from the uncracked to the cracked stage may be imperceptible. Thus suddenly the whole region adjacent to the cracked location becomes "disturbed". Over the length of the disturbed region, ℓ_D (Fig. 1d) the reinforcement a-bar strain is described by the solution of the bond (red distribution in Fig. 1d):

$$\varepsilon_{1.a}(x) = C_1 \cdot e^{-\omega x} + C_2 \cdot e^{\omega x}, \quad \omega = \sqrt{4 f_b^{\max} / (E_s D_b s_1)} \tag{A.2}$$

The solution of Eq. (A.2) is valid provided bond is in the elastic range (ascending branch in the bond slip law, Fig. 2c). Before the creation of a second crack, the following conditions characterize the end of the disturbed region at x= $\ell_{D,1.a}$:

i) the strain at x=0, $\varepsilon_{1.a}$ is known [=$I_{gr}/I_{cr}\cdot\varepsilon_{cr}$, ε_{cr} = $\varepsilon_{c.cr}\cdot y_{cg}/(0.5h)$ is the strain at the level of reinforcement when the concrete strain on the tension surface of the member is $\varepsilon_{c.cr}=f_{ct}/E_c\approx$0.00015]. Substituting in Eq. (A.2) it follows:

$$\varepsilon_{1.a} = C_1 + C_2 \tag{A.3a}$$

ii) the slope of the bar strain distribution, $d\varepsilon(x)/dx$, obtained from differentiation of Eq. (A.2), matches that of the strain diagram as would be obtained from Eq. (A.1) at some distance x=$\ell_{D,1.a}$<ℓ_o:

$$\omega \cdot \left(-C_1 \cdot e^{-\omega \ell_{D,1.a}} + C_2 \cdot e^{\omega \ell_{D,1.a}}\right) = -M_o y_{cg} / \left(E_c I_{gr} L_s\right) \tag{A.3b}$$

If Eq. (A.3b) is not satisfied, for x=$\ell_{D,1.a}$> ℓ_o, then use instead, $\varepsilon_{1.a}|_{x=\ell_D}$=0.

iii) bar strain $\varepsilon_{1.a}$ at x=$\ell_{D,1.a}$ satisfies both Eqs. (A.1-A.2):

$$\varepsilon_{1.a}\,|_{x=\ell_{D,1.a}} = \frac{M_o \cdot (1 - \ell_{D,1.a}/L_s)}{E_c \cdot I_{gr}} \cdot y_{cg} - \frac{N}{E_c \cdot A_g} = C_1 \cdot e^{-\omega \ell_{D,1.a}} + C_2 \cdot e^{\omega \ell_{D,1.a}} \tag{A.3c}$$

Unknowns of the system of Eqs. (A.3) are, the disturbed length $\ell_{D,1.a}$, and the coefficients C_1 and C_2. In an algorithm developed to solve Eqs. (A.3) numerically, the controlling parameter is $\varepsilon_{1.a}$ = $I_{gr}/I_{cr}\cdot\varepsilon_{cr}$ at x=0; required input includes the axial load, N, shear span L_s, the bond-slip characteristic property ω (Eq. A.2), and the member material and cross sectional properties. Coefficients C_1, C_2 are obtained from (A.3b) and (A.3c):

$$C_{1,2} = 0.5 \cdot e^{\beta \cdot \omega \cdot \ell_{D,1.a}} \left[\frac{M_o \cdot y_{cg}}{E_c \cdot I_{gr}} \cdot \left(1 - \frac{\ell_{D,1.a}}{L_s} + \frac{\beta}{\omega L_s}\right) - \frac{N}{E_c \cdot A_g} \right], \quad \beta = 1 \text{ for } C_1, \text{ and } \beta = -1 \text{ for } C_2 \tag{A.4}$$

Appendix B - The splice problem is analyzed for every bond stage separately in Table 1, and is always valid between the most inner cracks (ℓ_{int}, Fig. 2a) since the already formed flexural cracks require also splitting of the intermediate space. Parameter ℓ_{int} ranges between ℓ_o (considering only the end cracks, at M_o=M^{cr}) and ℓ_o-Σ($\ell_{1.a}^{cr.n}$ + $\ell_{1.e}^{cr.n}$) at cracking stabilization stage up until the splice failure. Along segments Σ($\ell_{1.a}^{cr.n}$ + $\ell_{1.e}^{cr.n}$) bar axial stress and strain remain constant because bond strength f_b^{max} due to cover is diminished (in the absence of confinement). (If confinement due to stirrups is present in the splitting segment, their contribution is considered in relieving the bar axial force through its contribution as residual bond strength, [11, 14].) In this sense, slip at the ends of ℓ_{int} as a result of bond solution in ℓ_{int} is progressively increased towards the end sections of ℓ_o by adding the product of constant strain times the associated cracked part (i.e., $\ell_{1.a}^{cr.n}$ for the members' base). From the top end splice cross section up to the tip (i.e, L_s-ℓ_o, Fig. 2) of the cantilever the reinforcing e-bars act as continuous reinforcement in the remaining shear span; there, the bar strain attenuation has been also connected with the bond mechanism [4]. The problem of the bars 1.a anchorage in the member's support (L_b^{eq} in Fig. 2) has already been demonstrated in [1-2]. These three bond solutions define the member's lumped drift due to pullout at the end sections of ℓ_o because the crack opening at these sections is owing to the sum of slip of reinforcement from both sides. For example, the crack opening at base, x=0, is the sum of slip of bar 1.a from the splice region ℓ_o and from anchorage L_b^{eq} and at x= ℓ_o is the sum of slip of bar 1.e from the splice region ℓ_o and from the remaining shear span L_s-ℓ_o. The solution of all three bond stages (Table 1) is demonstrated for the remotest and most critical tensile pair at first crack event (end cracks are formed due to attainment of cracking moment at base, M_o=M_{cr}) thus considering the entire length of available ℓ_o, i.e. ℓ_{int}= ℓ_o. However, by imposing incremental strain steps at member's base cracked cross section the implementation of Eqs. 2 precedes in defining the next crack event, i.e.

$\ell_{1.a}^{cr2}$ induced by bar 1.a. After localization of the second crack, and given the condition of splitting along $\ell_{1.a}^{cr2}$, strain ε_o at base is fully transmitted at $x=\ell_{1.a}^{cr2}$ for bar 1.a whereas for bar 1.e strain along $\ell_{1.a}^{cr2}$ is released and the bond solution is transferred to the available splice length $\ell_{int}= \ell_o - \ell_{1.a}^{cr2}$. Equations are given below only for the a-bar (similar equations hold for the e-bars with distance x measured from the top end of ℓ_o). For the intermediate crack state the bond solution is schematically depicted in Fig. 4.

Table 1 - Solving bond equation for different scenarios

Stage I: elastic bond ($s < s_1$, Fig. 2c) and elastic bar ($\varepsilon_o<\varepsilon_{sy}$, Fig. 2b)

Bars 1.a (distance x is measured from the base):

$$\varepsilon_{1.a}(x)=\frac{\varepsilon_o\left(e^{-\omega x}-e^{\omega(x-2\ell o)}\right)}{1-e^{-2\omega\ell_o}},\quad s_{1.a}(x)=\frac{\varepsilon_o\left(e^{-\omega x}+e^{\omega(x-2\ell o)}\right)}{\omega\cdot(1-e^{-2\omega\ell_o})},\ \omega^2=\frac{4f_b^{\max}}{D_bE_ss_1},\ f_b^{max}=\frac{2\mu}{\pi D_b}\left(p_{cr}\cdot\zeta\cdot f_{ct}\right)$$

The limit strain $\varepsilon^{el,I}$ beyond which bond enters in plastification stage II (attaining slip s_1, Fig. 2c): $\varepsilon^{el,I}=s_1\omega(1-e^{-2\omega\ell_o})/(1+e^{-2\omega\ell_o})<\varepsilon_{sy}$

Notes: a) In f_b^{max}: p_{cr} is the crack path of every pair, ζ quantifies the state of the concrete cover surrounding the pair (ζ=0.5 for thin cover, 2–3D_b, else ζ=1), μ is the coefficient of friction (0.9-1.2 for ribbed bars), f_{ct} is the concrete tensile strength (0.33-0.5$f_c^{0.5}$). Slip s_1 is an intrinsic property of the interface (0.1-0.2mm). The slip s_2 (Fig. 2c) is not a constant value [1]; for $\ell_o > \ell_{o,min}=D_bf_{sy}/(4f_b^{max})$ and bar strain at the initiation point equal to $\varepsilon_o=\varepsilon_{sy}+4\cdot(\ell_o-\ell_{b,min})\cdot f_b^{res}/(D_bE_{sh})$ assumes its maximum value as $s_2=s_1+0.5\ell_{o,min}\varepsilon_{sy}$. b) The crack width w_o at base (x=0) is the sum of slippage of bars 1.a from lap and the anchorage ($w_o=w_{\ell o}+w_{Lb}^{eq}$); the share from lap is $w_{\ell o}=(\varepsilon_o/\omega)\cdot(1+e^{-2\omega lo})\cdot(1-e^{-2\omega\ell_o})$ and the share from support (the bond solution at this stage is identical along the anchorage length L_b^{eq}, only bond property ω^* as per f_b^{max} may be altered) is $w_{Lb^{eq}}=(\varepsilon_o/\omega^*)\cdot(1+e^{-2\omega^*Lb^{eq}})\cdot(1-e^{-2\omega^*Lb^{eq}})$.

An approximate way to assess the lumped drift θ_{pull} at this stage is to divide w_o with the distance between neutral axis and bars 1.a, as $\theta_{pull}=w_o/y_1^{na}$.

Stage II: plastification of bond (s>s1, Fig. 2c) and elastic bar ($\varepsilon^{el,I}<\varepsilon_o<\varepsilon_{sy}$)

- Along the length of bond plastification, ℓ_p :

$$\varepsilon_{1.a}(x)=\varepsilon_o-4f_b^{\max}/(D_bE_s)\cdot x\ ,\ s_{1.a}(x)=s_1+0.5\cdot(l_p-x)\cdot\left(\varepsilon_{1.a}(x)+\varepsilon^{el,II}\right)\text{ with }\varepsilon^{el,II}=\varepsilon_o-4f_b^{\max}/(D_bE_s)\cdot\ell_p$$

$$\ell_p=\ell_o-\frac{1}{2\omega}\ln\frac{s_1\omega+\varepsilon^{el,II}}{s_1\omega-\varepsilon^{el,II}}$$

- Along the remaining length of the splice (individual ℓ_o-ℓ_p of each bar):

$$\varepsilon_{1.a}(x)=\frac{\varepsilon^{el,II}\left(e^{-\omega(x-\ell_p)}-e^{\omega(x-\ell_p)-2\omega(\ell_o-\ell_p)}\right)}{1-e^{-2\omega(\ell_o-\ell_p)}},\ s_{1.a}(x)=\frac{\varepsilon^{el,II}\left(e^{-\omega(x-\ell_p)}+e^{\omega(x-\ell_p)-2\omega(\ell_o-\ell_p)}\right)}{\omega\cdot\left(1-e^{-2\omega(\ell_o-\ell_p)}\right)}$$

The end of bond plastification coincides with yielding of reinforcement (i.e., $\varepsilon_{1.a}|_{x=0}=\varepsilon_{sy}$)

Stage III: debonding failure ($\varepsilon_o>\varepsilon_{sy}$)

ℓ_o comprises the sequence of the following segments: the yield penetration length ℓ_r (immediately adjacent to the support, where bond is equal to the residual value f_b^{res}), the bond plastification length ℓ_p (i.e. the length where the bar is elastic but bond is equal to f_b^{max}); Bar stress and bond stress are elastic in the remaining length (ℓ_o - ℓ_r - ℓ_p).

- Along the debonding length, ℓ_r ($f_b=f_b^{res}$):

$$\varepsilon_{1.a}(x)=\varepsilon_o-\frac{4f_b^{res}}{D_bE_{sh}}\cdot x\ ,\ s_{1.a}(x)=s_2+0.5\cdot\left(\ell_r-x\right)\cdot\left[\varepsilon_{1.a}(x)+\varepsilon_{sy}\right]$$

- Along the plastification length, ℓ_p ($f_b=f_b^{max}$):

$$\varepsilon_{1.a}(x)=\varepsilon_{sy}-\frac{4f_b^{\max}}{D_bE_s}\cdot\left(x-\ell_r\right),\ s_{1.a}(x)=s_1+0.5\cdot\left(\ell_r+\ell_p-x\right)\cdot\left[\varepsilon_{1.a}(x)+\varepsilon^{el,III}\right],\ \varepsilon^{el,III}=\varepsilon_{sy}-\frac{4f_b^{max}}{D_bE_s}\cdot\ell_p$$

- Along the remaining length (elastic bond, $f_b=f_b^{max}/s_1\cdot s(x)$):

$$\varepsilon_{1.a}(x)=\frac{\varepsilon^{el,III}\left(e^{-\omega(x-\ell_r-\ell_p)}-e^{\omega(x-\ell_r-\ell_p)-2\omega(\ell_o-\ell_r-\ell_p)}\right)}{1-e^{-2\omega(\ell_o-\ell_r-\ell_p)}}\ s_{1.a}(x)=\frac{\varepsilon^{el,III}\left(e^{-\omega(x-\ell_r-\ell_p)}+e^{\omega(x-\ell_r-\ell_p)-2\omega(\ell_o-\ell_r-\ell_p)}\right)}{\omega\cdot\left(1-e^{-2\omega(\ell_o-\ell_r-\ell_p)}\right)}$$

All boundary conditions for each bond stage are clearly depicted in Fig. 4.

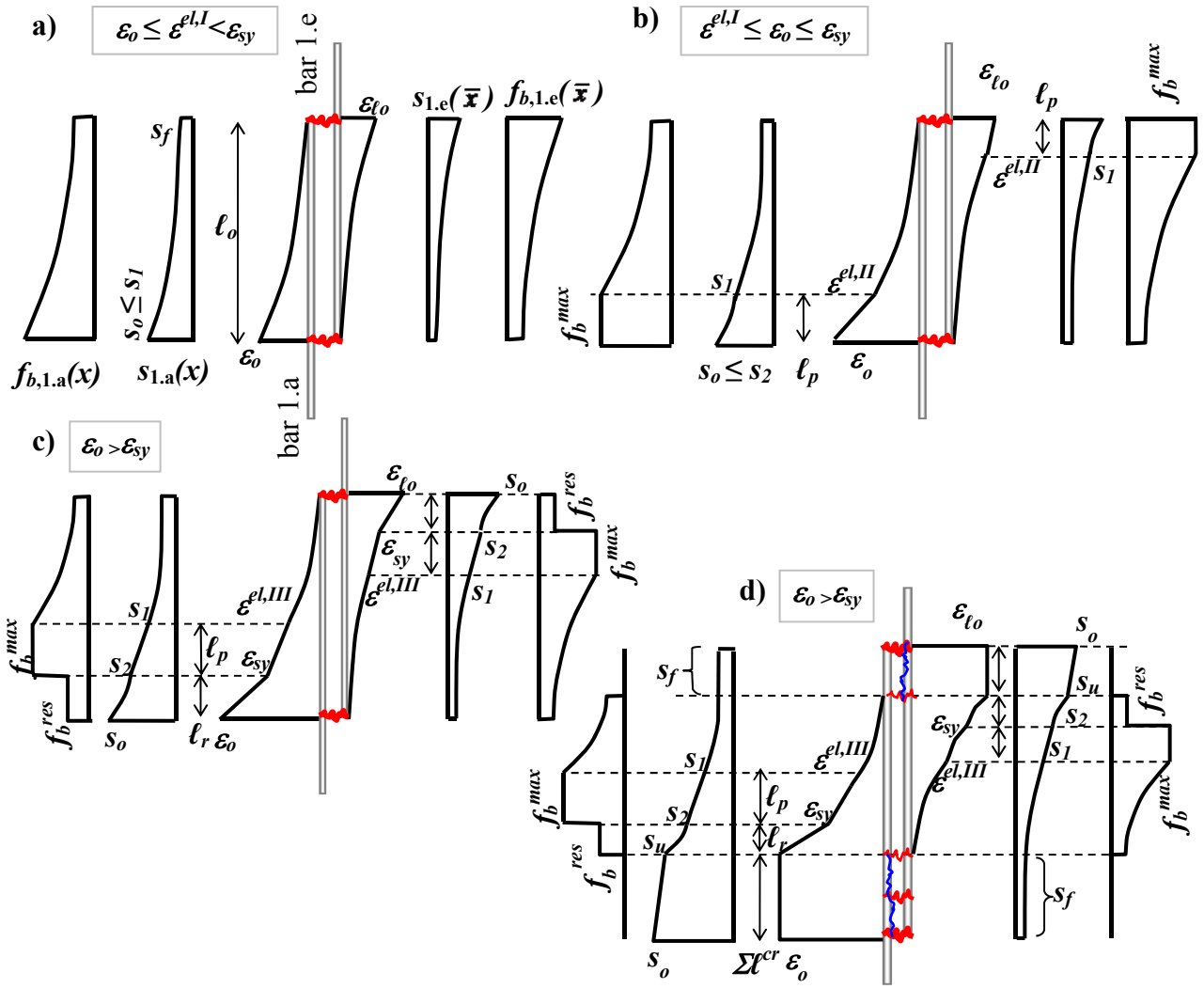

Fig. 4 - State determination of each bar of the pair (considering only end cracks) while bond-slip law a) remains elastic (Stage I), b) enters in the plastification region (Stage II) and c) fails due to debonding after yielding (Stage III). d) Stage III when inner cracks are formed.

